Experimental Investigation of Direct Liquid Cooling of a Two-Die package

Bharath Ramakrishnan[1], Sami Alkharabsheh[1], Yaser Hadad[1], Paul R. Chiarot[1]
Kanad Ghose[1], Bahgat Sammakia[1], Vadim Gektin[2], Wang Chao[3]
[1]State University of New York at Binghamton, Binghamton, NY, 13902, USA
[2]Futurewei Technologies, Santa Clara, CA, 95050, USA
[3]Huawei Technologies, Shenzhen, Guangdong, PRC, 518129
Email: bramakr1@binghamton.edu

Abstract

Recent commercial efforts have reestablished the benefits of cooling server modules using direct liquid cooling (DLC) technology. The primary drivers behind this technology are the increase in chip densities and the absolute need to reduce the overall data center power usage. In DLC technology, a cold plate is situated on top of the chip with thermal interface material between the chip and the cold plate. The low thermal resistance path facilitates the use of warm water which helps data centers in replacing the chilled water system by a water side economizer utilizing ambient temperature. This work describes the effort to leverage DLC by employing microchannel cold plates to cool multi-chip modules. The primary objective of this work is to build a sophisticated test rig to characterize the flow and thermal performance of a microchannel cold plate for cooling a two-die chip. This study highlights the challenges of building an experimental setup which simulates a two-die chip package and the approaches taken to overcome the challenges. A parallel channel cold plate is used to benchmark the performance. Tests were conducted for a set of independent variables like flow rate, input power to dice, coolant temperature, flow direction and TIM resistance. The results are presented as PQ curves, specific thermal resistance curves and case temperature distribution reflecting the effect of changing the input variables.

Keywords

Direct liquid cooling, warm water cooling, microchannels, cold plate, specific thermal resistance, heat transfer coefficient, flow direction

Nomenclature

TIM	Thermal Interface Material
MCM	Multi-Chip Module
IHS	Integrated Heat Spreader
lpm	liters per minute
ΔT	Temperature difference
T_{in}	Inlet temperature
T_{out}	Outlet temperature
Q_w	Heat picked by the coolant
$\dot{m}$	Mass flow rate of the coolant
C_p	Specific heat of the coolant
R_{th}	Specific thermal resistance [°C.cm^2/W]
T_{case}	Case temperature [°C]

1. Introduction

Over the last two decades, researchers around the world are investing a significant amount of time and money to create faster computers which can give them an edge in the global market. 'How fast the computer can perform is directly related to how cool it can be kept'. A data center is nothing but a scaled up version of several computers stacked together in a particular fashion. The Information and Communication Technology (ICT) infrastructure power usage breakdown shows that the data centers in U.S are consuming power at an alarming rate of 150TWh [1]. While 50% of the power consumed by data centers goes towards cooling with major consumption from computer room air conditioning (CRAC). The demand for data centers are only going to ramp up as people connect more and more for both social and economic reasons. There is a dire need to limit the power spent towards cooling while also remembering the growing scarcity in natural resources for power production.

The idea of forced convection using liquid to cool chips is not a new technique. In 1981, Tuckerman and Pease [2] investigated the idea of using liquid in cooling a processor chip by etching channels on the back of silicon wafer. Several works were carried out on the numerical investigation and optimization of microchannel heat sinks [3, 4]. Experimental study of stacked microchannel heat sink for cooling of microelectronic devices was performed by Wei et al. [5]. Effect of coolant flow direction and flow rate ratio was investigated in each microchannel layer. A total resistance of about 0.09 °C/(W/cm^2) was observed for parallel and counter flow configurations. It was concluded that the flow ratio between the top and bottom layer can be customized to achieve lower pumping power while the effect of partial and uniform heating were also discussed in identifying the local hot spots especially for higher flow rate conditions. Kandlikar et al. [6] evaluated various techniques of single phase flow in microchannels for high heat flux chip cooling in an attempt to enhance the thermohydraulic performance. The performance was augmented in many ways like by using an enhanced fin design or by breaking the boundary layer through flow constrictions or incorporation of mixing devices to enable mixing between bulk fluid and channel walls. Cold plate prototypes which incorporate several of the above mentioned enhancement techniques were tested while the current work focuses on the performance of a cold plate with parallel channels.

Jie Wei [7] discussed the many challenges in cooling used for high performance servers especially the MCM. The advantage of using an integrated heat spreader (IHS) was discussed as IHS can help in spreading the heat from the chip to a wider area and thus minimizing the on chip temperature gradient caused by asymmetric power

distribution. Also presented were results from using liquid cooled MCM package which uses liquid spray impingement technology for Fujitsu high end server GS8900. Wei also discussed the many advantages of using an advanced TIM in minimizing the interfacial resistances between the chip and its heat spreader and/or to a heat sink. Novel graphite based TIM was tested in the current study in an attempt to bring down the overall thermal resistance.

Charlotte et al. [8] experimented with an integrated heat sink for a power MCM by developing a 3-D approach. The tested MCM has 4 elementary modules with two IGBT chips in each module. A total thermal resistance value was obtained by averaging the eight chip thermal resistances for several values of dissipated power. A thermal resistance value between 0.09-0.11 K/W with no significant variation in the range of power to the chip was reported. While the pressure drop between the incoming and outgoing fluid were reported for several flow rate values, its impact on thermal resistance was also studied. Kim et al. [9] studied the thermal management of liquid cooled cold plates for six heat sources in a humanoid robot for both serial and parallel configuration. Six copper heating blocks of size 10mm x 10mm x 8.5mm was used to simulate six heat generating chips inside a humanoid robot. Variables tested were input power to the heating blocks, flow rates and water temperature. It was found that the two-way parallel configuration proved to be the effective cooling method because in the series configuration the surface temperature rise from the first chip to the last chip is higher than that of parallel configuration for the same flow rate condition tested. Literatures [10] and [11] proposed several methodologies to evaluate the thermal performance of MCM considering the number of dice, their locations in the board and associated power with it.

The performance of a microchannel heat sink/cold plate in an actual server from an actual rack can be studied by real time measurement of coolant flow rates, coolant temperatures in and out of the cold plate, and the actual chip temperature. A recent study from Alkharabsheh et al. [12] found that servers account for 56% of total pressure drop in a DLC rack, while 69% of the modules pressure drop goes towards the plumbing which includes hoses and quick connects. Therefore, a properly designed heat sink will not only have high heat transfer coefficient but also minimal pressure drop as larger pressure drop results in higher pumping power. Although the net aim is to improve the overall energy efficiency of warm water cooling for the data center, the focus of this work is on characterizing, optimizing and improving the performance of the cold plate designed to address multiple hot spots. By setting up a bench level experiment, the researcher would have capability on varying the operational parameters such as coolant temperature, chip power and coolant flow rate. While different microchannel geometries were explored to increase the convection efficiency, the scope the current work is restricted to a cold plate design with parallel microchannels. The results obtained from the parallel microchannel design can set the benchmark for validating the performance of other intuitive microchannel designs. This paper also addresses the many challenges associated with setting up an experimental setup to simulate a multi-die package and the steps taken to overcome them.

2. Bench Level Experimental Setup

Building an experimental setup to simulate a two-die chip package revealed practical challenges compared with common test setups used for a single die package. This section describes the experimental setup for thermal evaluation of a cold plate used for two-die chip cooling. Details of fixture for mock chips, internal heat spreader (IHS) or case/lid details, cold plate design and geometry, and procedures to assemble cold plates on top of the heat spreader are discussed. The fixture is constructed in such a way that it can accommodate any cold plate of interest. Detailed information on the list of instruments used in this study and their associated accuracy are also discussed in this section.

2.1 Mock Package

The packaging industry with its next generation of processors will have several dice in a single package. A Node's package with a total size of 64.29mm x 41.2mm was used in this study. The chosen package has two dice respectively; SKX (skylake) die and FPGA die. The dice can dissipate a total power of up to 300W. The particular layout was chosen such that the cold plate's internal construction should be able to address multiple (2) hot spots. An actual package has several layers of intricacies starting from the substrate in the bottom to the Integrated Heat Spreader (IHS) on top with layers of thermal interface material in between them. A rigid test fixture was developed to simulate a mock package with different layers as shown in Figure 1.

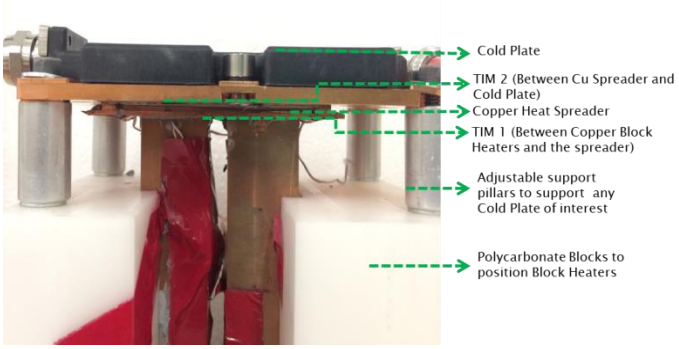

Figure 1: Test fixture assembly showing the cold plates installed on top of copper block heaters with integrated heat spreader and thermal grease between them

Cross sectional area of SKX and FPGA dice are 20.58mm x 31.04mm and 20.58mm x 15.47mm respectively. Two copper blocks with a total height of 108mm and cross sectional areas corresponding to the dice

were used as mock chips in this study. Cartridge heaters (Omega-CIR-1014/120V) with dimensions of 6.3mm OD and 31.8mm sheath length, and a wattage density of 40 W/cm^2 were used to heat the copper blocks. SKX and FPGA die contain 4 and 2 cartridge heaters respectively. The cartridge heaters can be powered individually using power supplies (Sorenson DCS-100-10E). Three RTDs were installed across each copper block heaters to measure the temperature gradient. The RTD temperatures were recorded using DAS Module NI 9219. The entire setup was thoroughly insulated on all the sides leaving out the top surface on the copper block heaters such that the heat flows in 1-D. Low conducting polycarbonate blocks were used to position copper block heaters. All the components were fabricated with as tight machining tolerance possible. Surface flatness was ensured using a flatness indicator at different stages of fabrication and assembly.

An integrated heat spreader (IHS) made of copper was installed on top of the dice. A heat spreader was desired as it spreads the heat from the chip to a wider area thus minimizing the on-chip temperature gradient caused by uneven power distribution [7]. The heat spreader is typically 2-10 times bigger than that of the die size and act as first level conduction spreader. The heat spreader was installed on top of the dice with thermal grease at the interface. The heat spreader temperature is referred to as 'case temperature' in the sections to follow. Five T-type thermocouples named A-E were installed on top of the spreader to represent case temperatures. Figure 2 is the planar view showing the arrangement of thermocouples on top of the heat spreader relative to the dice.

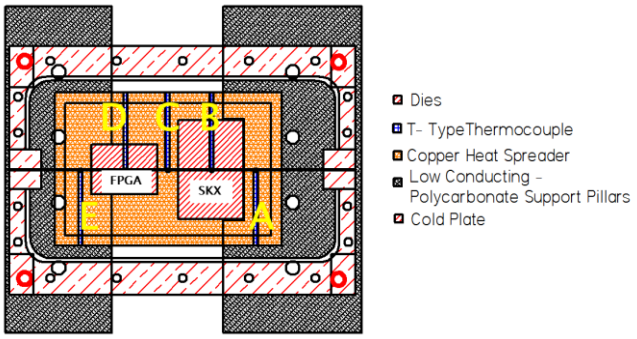

Figure 2: Planar view showing the arrangement of T-type thermocouples and their position with respect to the dice and the internal heat spreader

Thermocouples B and D were installed right on top of SKX and FPGA die locations respectively with thermocouple C in between them. Thermocouples A and E are located outside the die area at the fluid inlet and exit locations respectively. The laboratory made T-type thermocouples were calibrated using a precision oven and a linear calibration curve was obtained between each thermocouple and oven temperature. Thermocouple readings were measured using DAS module NI-9219.

2.2 Tested Cold Plate

The overall aim of this work is to build a cold plate with microchannels while maintaining a thin profile designed to address two hot spots. Thin profile of cold plates support high density systems like 1U or blade chassis. Figure 3 shows the cold plate tested in this study which can be employed in a typical data center server rack which uses warm water DLCS (Direct Liquid Cooling System). The dimensions of the cold plate are 108mm x 72mm x 11.5mm. The cold plate has two main parts; base part made of copper containing the microchannels and the plastic cover part. The plastic cover part contains the inlet and exit manifolds to carry the coolant in and out of the microchannels. The cold plate was designed with total height of 11.5mm (including that of base part and the plastic cover part) to accommodate lower profile footprints like blade servers or custom chasses. The base part has a thickness of 3.5mm and act as a second level conduction spreader. The fin pitch is 200 µm and the fin thickness is 150 µm with a total number of 135 channels. The cold plate has parallel microchannels through its length. The thermal behavior of parallel channel cold plates are well established in literature and are used for verifying the results obtained from tests.

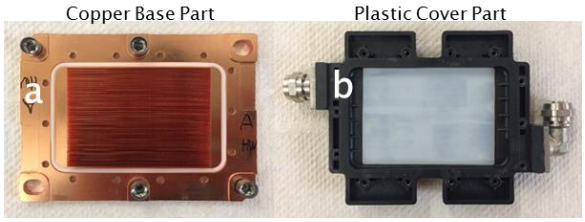

Figure 3: The tested cold plate showing (a) the copper base part containing the microchannels (b) the plastic cover part containing the inlet and exit manifolds

2.3 Assembly Procedures

Assembling the heat spreader on to the dice and then the cold plate on top of heat spreader is an important step performed with utmost care prior to running the tests. Uneven assembly would result in formation of air voids at the interface adding to the contact resistances and thus hindering the thermal resistance measurements. The heat spreader with thermocouples is mounted on top of the dice with thermal grease (Shin Etsu-X23-7783D) at the interface. A constant load is applied to this arrangement for nearly 2 hours before installing the cold plate. The cold plate is then assembled on top of the heat spreader (IHS) with the second layer of thermal interface material between them. Cold plates are mounted by tightening the screws on the four corners of the cold plate. A torque wrench was used to deliver uniform torqueing while a crisscross mounting

pattern was followed ensuring even distribution of load. The mounting procedure was qualified by assembling a lexan plate (with the dimensions of an actual cold plate) on to the dice with TIM in between them. Obtained microscopic images at the interface indicate no formation of voids by following the above mentioned mounting procedure. The entire set up is thoroughly insulated to minimize any heat loss to the surroundings.

The schematic of the experimental setup is as shown in Figure 4. DI water stored in the reservoir is driven through the loop using a precision geared pump (Cole Parmer EW-73004-02) with a magnetic drive (EW-07144-91). A laboratory made flow controller with needle valves was used to control the flow rate precisely. The flow through the loop was measured using a flow meter (Omega-FTB 313D) with a full scale accuracy of ±6%. The tested velocities are in the range where the erosion is not a concern in the microchannels. A 20um water filter was used to filter out any particulates getting into the microchannels. The coolant temperature was precisely maintained using a liquid-liquid heat exchanger. A Julabo chiller (LH 40) which uses special oil with a working temperature range of -45°C to 250°C was used to control the inlet coolant temperature. Two custom made copper block arrangements with provisions to measure the temperature and pressure were stationed at the inlet and the exit of the cold plate assembly. RTDs were employed to measure the coolant temperatures at the inlet and exit. The RTD temperatures were recorded using DAS Module NI 9219. The pressure drop across the cold plate was measured using a pressure transducer (PX-2300). The pressure drop variations were recorded as current signals using DAS Module NI-USB-6001. LabVIEW was programmed to measure/write the temperature and pressure data.

3. Results and Discussion

Experiments were categorized into two sections namely; 1. Flow resistance experiments (PQ Tests) and 2. Thermal resistance experiments (case temperature measurements).

3.1 Flow Resistance Experiments

Flow resistance experiments were conducted to measure the pressure drop across the cold plate which includes the pressure drop in the inlet, exit manifolds and that of the microchannels. A pressure transducer used has an accuracy of ±0.25% RSS. Each tests were performed twice for the exact operating conditions and good repeatability was observed. The primary independent variables were flow rate and coolant temperature. The cold plate is laid out in the bench to avoid any bends in the hoses getting in and out of the cold plate as any bend would account for an irrelevant drop. The coolant temperature was set to 27°C and the flow rate was varied from 0.35 lpm to a maximum value of 1.0 lpm in small steps and the pressure drop value was recorded after giving sufficient time at each step. Results shown in Figure 5 represent a pressure drop value of 6.7 kPa at the maximum flow rate tested.

Tests were extended to a higher coolant temperature value of 55°C by controlling the chiller. It was observed that the coolant temperature plays a crucial part in pressure drop findings. The pressure drop across the cold plate decreases by 18% when the coolant temperature was increased as shown in Figure 5. This is due to the drop in viscosity of the coolant with rise in coolant temperature. Though the results from the thermal tests (discussed in subsequent sections) reveal that the cold plate heat transfer characteristics/thermal performance does not improve with coolant temperature, PQ tests indicate that, it is advantageous to operate the cold plate at a higher inlet coolant temperature as it reduces the pumping power. This result adds credit to the concept of 'warm water cooling'.

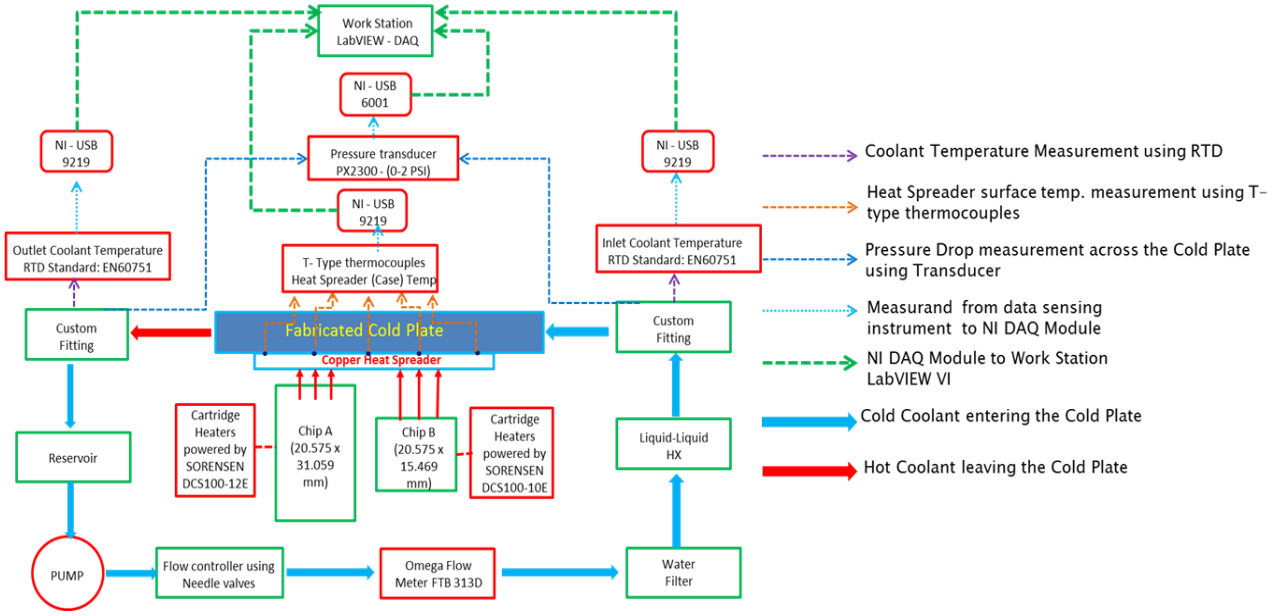

Figure 4: Schematic of the experimental setup

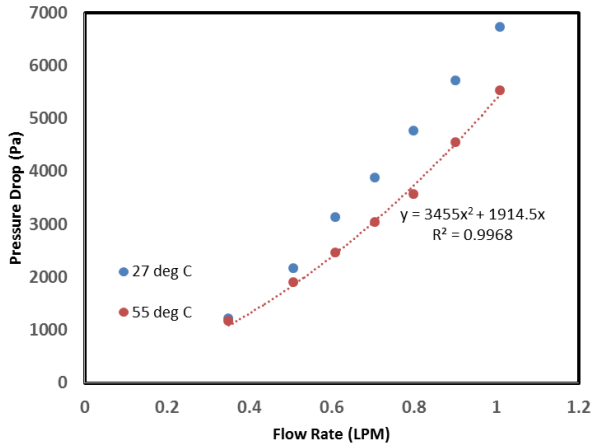

Figure 5: PQ test comparison showing the effect of coolant temperature on pressure drop

3.2 Thermal Resistance Experiments

Thermal resistance experiments were performed to observe the thermal performance of the cold plate at different primary independent variables like coolant temperature, coolant flow rate and die power. Tests were conducted to identify the specific thermal resistance based on individual case temperatures.

3.2.1 Experimental Procedure

The coolant temperature was set at 29°C using the external chiller unit. The flow rate was precisely controlled by adjusting the power to gear pump. Flow rates were maintained at 0.35 lpm, 0.60 lpm, 0.80 lpm and 1.0 lpm for the set of tests discussed in this paper. Power to SKX die was varied from 50-100-150-210W while the power to FPGA die was maintained constantly at 90 W. Thus a maximum power of 300W was tested. Case temperature data was recorded for each power load after giving sufficient time for the system to reach steady state. Tests were conducted by closely monitoring the operating parameters while also providing a thorough insulation to the system to minimize any heat loss. Figure 6 presents the energy balance comparison obtained between the input and output power to show the efficacy of the experimental results.

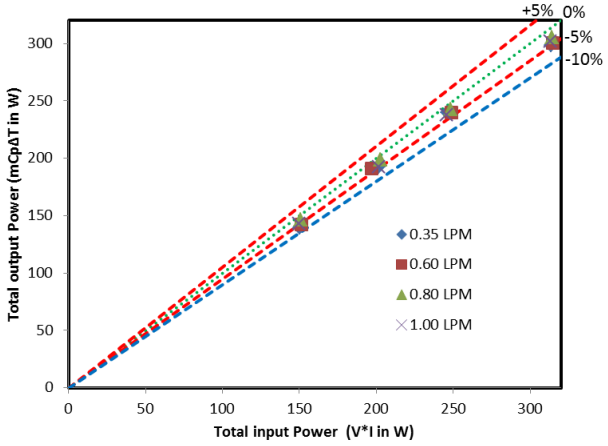

Figure 6: Energy balance comparison between input and output power at different flow rates

Input power was calculated using voltage (V) and current (I) data obtained from power supply while the output power was calculated using $Q_w = mC_p(T_{out} - T_{in})$. Obtained results indicate a heat loss of less than ±5% with the setup. But in an actual scenario, there would be a significant amount of heat loss from the dice to the board and other components in the form the conduction. The case temperatures value reported here are thus higher than what would be expected in real application.

3.2.2 Specific Thermal Resistance

The plots shown in the Figure 7 are marked in alphabets 'a-d' to represent four scenarios where the power to the bigger die was varied as 50 W, 100 W, 150 W and 210 W respectively while the power to smaller die was maintained constantly at 90 W. Figure 7 shows the temperature measurements on the heat spreader surface as the power to the dice and flow rate were varied. As the flow rate was increased, the case temperature value dropped down. The amount of drop in temperature was sginificant as the flow rate was changed from 0.35 to 0.6 lpm. But the drop in case temperature readings was minimal as the flow rate was changed from 0.80 to 1.0 lpm. This translates as, the thermal resistance drops with rise in flow rate and reaches a constant value, changing the flow rate any further do not have a significant impact on the thermal performance. In other words the heat transfer coefficient is increasing and moving towards a saturation value as the coolant flow rate is increased from 0.35 to 1.0 lpm. The specific thermal resistance and heat transfer coefficient calulations are reported in the sections to follow.

Test conducted at a higher coolant flow rate value of 1.2 lpm also suggested the loss in efficient convection with increase in flow rate above 1 lpm as shown in the Figure 8. The results were compared at different flow rates for the case when the maximum power of 300 W was delivered to the dice. 210W to SKX die and 90W to FPGA die was delivered at an inlet coolant temperature value of 29°C. The coolant outlet temperature reaching a constant value suggests saturation in convection process. Increasing the flow rate any further will be a penalty in terms of pumping power.

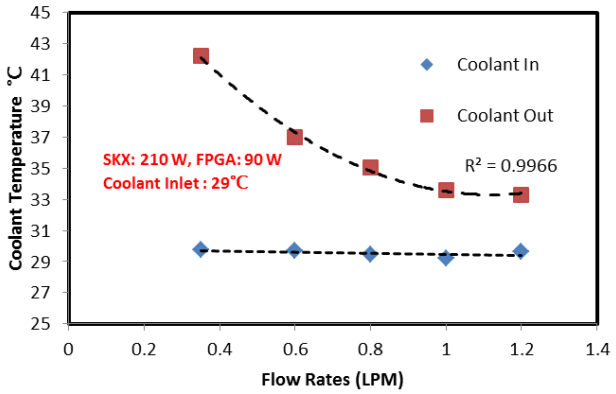

Figure 8: Variation in the coolant temperature at different flow rates for the case when 210 W and 90W was delivered to die 1 and die 2 respectively

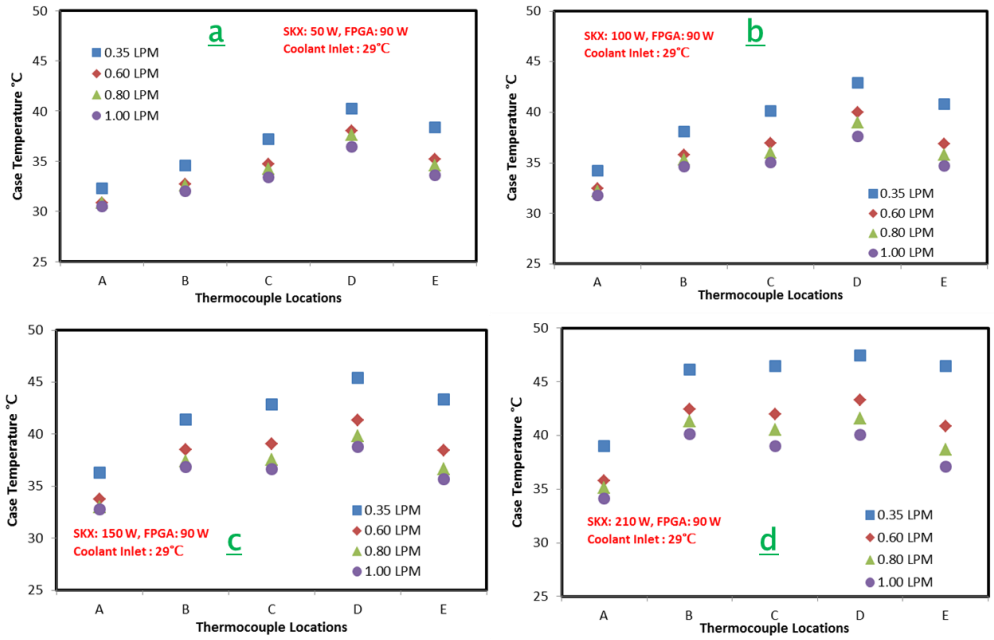

Figure 7: Case temperature distribution with respect to change in input power and flow rate

A specific thermal resistance value plot as shown in Figure 9 was generated based on the case temperatures corresponding to thermocouple locations B and D, in other words, case temperatures corresponding to SKX and FPGA dice. The specific thermal resistance is defined as

$$\boldsymbol{R}_{\text{th\_B}} = \frac{T_{case,B} - T_{in}}{Q''_{SKX}}, \boldsymbol{R}_{\text{th\_D}} = \frac{T_{case,D} - T_{in}}{Q''_{FPGA}}$$

where T_{case_B} and T_{case_D} represent case temperature with respect to SKX and FPGA at thermocouple locations B and D. T_{in} represent the inlet coolant temperature. Q''_{die} represents heat flux corresponding to respective dice. The uncertainty in specific thermal resistance measurement was estimated to be ±8%.

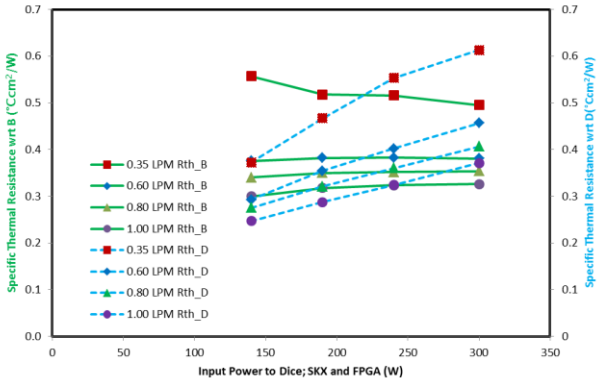

Figure 9: Specific thermal resistance with respect to change in input power to respective dice and flow rate at a coolant temperature of 29°C

At a constant flow rate, the specific thermal resistance R_{th_B} did not change with input power. This was expected as the cold plates thermal resistance should not alter to variation in input power to chips. While the specific thermal resistance R_{th_D} die increases linearly. R_{th_D} is defined based on the reference inlet temperature value of 29°C as the actual inlet temperature of coolant reaching the FPGA die from SKX die area is not measured in the test. Thus R_{th_D} go up due to rise in T_{case_D}. At a particular flow rate, averaging the specific thermal resistance values obtained with respect to FPGA die, R_{th_D} at different input power matches with the constant value of specific thermal resistance calculated with respect to SKX die, R_{th_B}. These results corroborate to the fact that the cold plate's thermal performance should not change to variations in input power to dice. At the lowest power level (50 W to SKX die and 90 W to FPGA die) and at the lowest flow rate (0.35 lpm) tested, the case temperature B is influenced by power to FPGA die. Meaning, there is good amount of conduction/spreading at the lower power level and when the flow rate is low. As the flow rate is increased, convection becomes the more dominant heat transfer mechanism; hence the specific thermal resistance does not change with input power to SKX die at flow rates of 0.60 lpm and above. Heat transfer coefficient (h) was estimated from the average specific thermal resistance as shown in Figure 10.

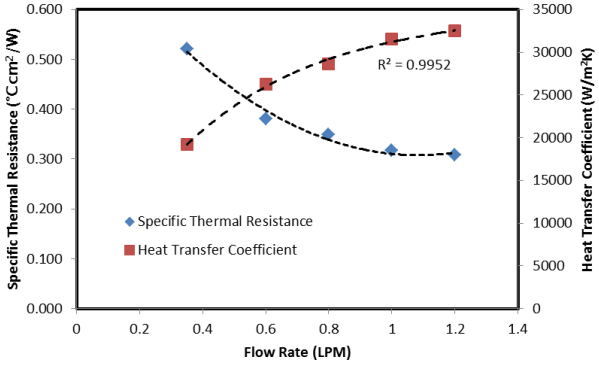

Figure 10: Variation in specific thermal resistance and heat transfer coefficient with respect to the flow rates

Heat transfer coefficient (h) reach a saturation value as the flow rate is increased above 1.00 lpm. Heat transfer coefficient (h) at the maximum flow rate tested was estimated to be about 30000 W/m^2.K. These results are consistent with published data for water cooled microchannel cold plates. The result also confirm with an earlier statement suggesting loss in convective efficiency with increase in flow rate.

3.2.3 Effect of changing coolant temperature

In an actual data center which has adopted warm water cooling system (DLCS), coolant would be at a higher temperature thus avoiding the need for an external chiller. The excess heat extracted from the heated coolant leaving the server can be used in several ways like space heating. An experiment was conducted at a higher inlet coolant temperature of 59°C by adjusting the external chiller unit. Figure 11 compares the case temperature distribution at two different inlet coolant temperatures 29°C and 59°C for a flow rate of 1 lpm and a maximum power of 300 W to the dice. Results show that the case temperatures increase linearly with increase in coolant temperature, suggesting that the heat transfer characteristics do not improve with rise in coolant temperature, as expected. At the same time, pressure drop results obtained at a higher coolant temperature translate to lesser pumping power as reported earlier. The case temperature values corresponding to SKX and FPGA dice are 70.7°C and 70.8°C respectively.

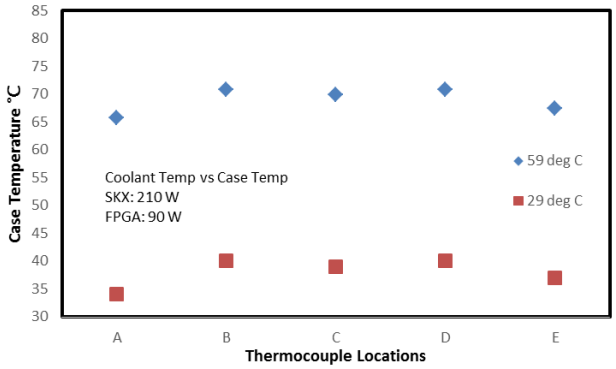

Figure 11: Comparison of case temperature distribution at two different coolant temperatures 29°C and 59°C, when the power to the dice is 300 W and coolant flow rate is 1 lpm

3.2.4 Effect of changing coolant flow direction

Results reported in the earlier sections are when the inlet is near the SKX die or thermocoiple location A in IHS. Tests were conducted after changing the flow direction in the microchannels with the inlet near the FPGA die or thermocouple location E in the heat spreader. Results shown in Figure 12 compares the effect of changing flow direction. Tests were conducted at a flow rate of 1 lpm and when the power to the dice is 300W. Obtained results indicate that by changing the flow direction from A-E to E-A, the case temperature with respect to FPGA die drops significantly by about 3.8°C. While a quick model calculation performed when the flow direction is A-E, assuming all the heat from SKX die is picked by the incoming coolant, reveal that the higher case temperature value with respect to FPGA die is because of the heated coolant leaving SKX die and not due to conduction or spreading. These results are especially good as they not only show the effect of neighboring dice on each other but also let the board developers decide how closely the dice can be positioned to each other as the interconnect length plays a crucial part in data transmission/retrieval time.

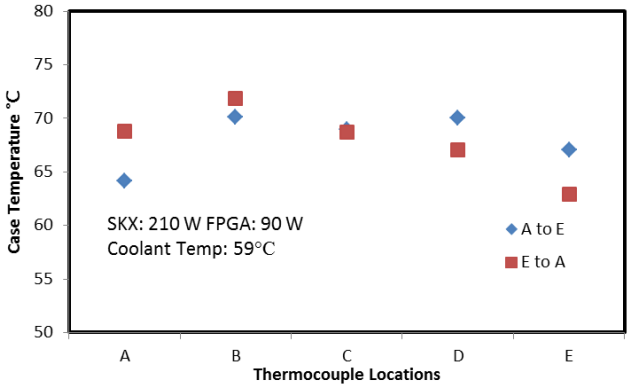

Figure 12: Case temperature distribution comparing the effect of change in coolant flow direction.

3.2.5 Effect of changing TIM

Experiments were conducted using an advanced TIM HT-C3200 to show that the efficiency of liquid cooling can be improved using an enhanced TIM. The tested thermal interface material is first of its kind, a compressible graphite sheet with a thermal conductivity of 7.8 W/mK compared to a thermal conductivity value of 6.0 W/mK for the thermal grease used in the earlier set of experiments. Tests were conducted at an inlet coolant temperature of 29°C and with power to SKX die and FPGA die as 210W and 90W respectively. The obtained case temperature values were compared with that of using thermal grease as shown in the Figure 13. The average case temperature value drop by about a 1.5°C by the use of graphite sheet as TIM.

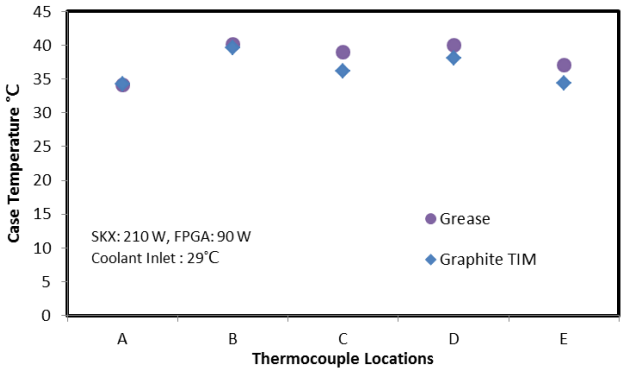

Figure 13: Comparison of case temperature distribution using two different TIM materials

4. Conclusions

A sophisticated bench level experiment was devised and built to characterize the flow and thermal performance of a warm water cooled cold plate used for two-chip thermal management. The setup is thoroughly insulated with about 5% of heat loss to ambient. The independent variables in the tests

were flow rate, coolant temperature, coolant flow direction, input power to the dice and the TIM.

PQ tests performed at a flow rate of 1lpm and at two different inlet temperatures 27°C and 55°C indicating that the pressure drop decreases by 18% as the coolant temperature is increased. Input power to the dice was varied at different coolant flow rates and the case temperature distribution was observed. It was found that the case temperature values drop significantly as the coolant flow rate is increased from 0.35 0.6 lpm and the drop ceases as the coolant flow rate is moved from 0.8 to 1.0 lpm suggesting saturation in efficient convection. Specific thermal resistance with respect to the dice were calculated based on the obtained case temperature values and it was observed that the specific thermal resistance do not change with input power and the resistance value drops with increase in flow rate. A heat transfer coefficient value of 30000 W/m^2K was estimated at the maximum flow rate and power to the dice.

Experiments conducted at a higher coolant temperature show that the case temperature values rise linearly with coolant temperature suggesting no improvement in the thermal performance. While tests conducted after changing the flow direction hint that it is advantageous to let the FPGA die receive the coolant first and looking at the results in an intuitive fashion can let the board designers decide how closely the chips can be placed with respect to each other. Tests were extended to the use of a graphite sheet TIM. Average case temperature drops by 1.5°C by the use of an advanced TIM compared to the traditional thermal grease.

Experimental results characterizing the performance of a microchannel cold plate for MCM cooling are especially good as they set the benchmark for other innovative microchannel geometry and design which can then be validated and optimized through numerical simulation. The study was extended to different microchannel designs and would be reported in later articles from the authors.

Acknowledgements

This work is supported by NSF IUCRC Award NO. IIP-1134867. The author would like to thank Pat Crowley and Ron from Progressive Tool Co, Endwell, NY for their guidance and assistance in putting the mock package together.

References

1. Mills, Mark P., “The Cloud Begins with Coal,” August 2013, Available: http://www.tech-pundit.com
2. D. B. Tuckerman and R. F. W. Pease, "High-performance heat sinking for VLSI," in IEEE Electron Device Letters, vol. 2, no. 5, pp. 126-129, May 1981.
3. R. W. Knight, D. J. Hall, J. S. Goodling and R. C. Jaeger, "Heat sink optimization with application to microchannels," in IEEE Transactions on Components, Hybrids, and Manufacturing Technology, vol. 15, no. 5, pp. 832-842, Oct 1992.
4. D. Copeland, "Optimization of parallel plate heatsinks for forced convection," Sixteenth Annual IEEE Semiconductor Thermal Measurement and Management Symposium (Cat. No.00CH37068), San Jose, CA, 2000, pp. 266-272
5. Wei X, Joshi Y, Patterson MK. Experimental and Numerical Study of a Stacked Microchannel Heat Sink for Liquid Cooling of Microelectronic Devices. ASME. J. Heat Transfer. 2007;129(10):1432-1444.
6. Kandlikar SG, Grande WJ. Evaluation of Single Phase Flow in Microchannels for High Flux Chip Cooling: Thermohydraulic Performance Enhancement and Fabrication Technology. ASME. International Conference on Nanochannels, Microchannels, and Minichannels, ASME 2nd International Conference on Microchannels and Minichannels ():67-76.
7. Wei J. Challenges in Package Cooling of High Performance Servers. ASME. International Electronic Packaging Technical Conference and Exhibition, ASME 2007 InterPACK Conference, Volume 2 ():501-507.
8. C. Gillot, C. Schaeffer and A. Bricard, "Integrated micro heat sink for power multichip module," in IEEE Transactions on Industry Applications, vol. 36, no. 1, pp. 217-221, Jan/Feb 2000.
9. Seo Young Kim, Kyudae Hwang, Jongmin Moon and Sarng Woo Karng, "Thermal management of liquid-cooled cold plates for multiple heat sources in a humanoid robot," 2009 4th International Microsystems, Packaging, Assembly and Circuits Technology Conference, Taipei, 2009, pp. 453-456.
10. B. S. Lall, B. M. Guenin and R. J. Molnar, "Methodology for thermal evaluation of multichip modules," Proceedings of 1995 IEEE/CPMT 11th Semiconductor Thermal Measurement and Management Symposium (SEMI-THERM), San Jose, CA, 1995, pp. 72-79.
11. C. D. Patel, "Backside cooling solution for high power flip chip multi-chip modules," 1994 Proceedings. 44th Electronic Components and Technology Conference, Washington, DC, 1994, pp. 442-449.
12. S. Alkharabsheh, B. Ramakrishnan and B. Sammakia, "Pressure drop analysis of direct liquid cooled (DLC) rack," 2017 16th IEEE Intersociety Conference on Thermal and Thermomechanical Phenomena in Electronic Systems (ITherm), Orlando, FL, 2017, pp. 815-823.
13. M. Hoffmeyer, P. Subramanian, R. Beyerle and P. Mann, "Novel graphite-based TIM for high performance computing," 2017 16th IEEE Intersociety Conference on Thermal and Thermomechanical Phenomena in Electronic Systems (ITherm), Orlando, FL, 2017, pp. 243-250.